Roll-to-roll fabricated lab-on-a-chip devices

2011 J. Micromech. Microeng. 21 035006

(http://iopscience.iop.org/0960-1317/21/3/035006)

J. Micromech. Microeng. **21** (2011) 035006 (6pp) doi:10.1088/0960-1317/21/3/035006

Roll-to-roll fabricated lab-on-a-chip devices

Asger Laurberg Vig[1], Tapio Mäkelä[2,3], Päivi Majander[2], Vito Lambertini[4], Jouni Ahopelto[2] and Andrs Kristensen[1,5]

[1] DTU Nanotech, Department of Micro and Nanotechnology, Technical University of Denmark (DTU), Building 345east, Oersted Plads, DK-2800 Lyngby, Denmark
[2] VTT Micro and Nanoelectronics, PO Box 1000, FIN-02044 VTT Espoo, Finland
[3] Funmat center, Åbo Akademi University, FI-20500 Turku, Finland
[4] Advanched Manufacturing and Materials Micro and Nanotechnology, Centro Ricerche Fiat S.C.p.A, Strada Torino 50, 10043 Orbassano, Italy

E-mail: Anders.Kristensen@nanotech.dtu.dk

Received 13 October 2010, in final form 6 January 2011
Published 3 February 2011
Online at stacks.iop.org/JMM/21/035006

Abstract
We present a high-volume fabrication technique for making polymer lab-on-a-chip devices. Microfluidic separation devices, relying on pinched flow fraction, are roll-to-roll fabricated in a cellulose acetate (CA) film at a volume of 360 devices h^{-1} for a cost of approximately 0.5 euro/device. The manufacturing process consists of two steps: (i) roll-to-roll thermal nanoimprint for patterning the microchannels into a CA film and (ii) roll-to-roll lamination for bonding another CA film onto the imprinted film to seal the microchannels. Reverse gravure coating is used to apply an adhesive polymer onto the CA lid film before roll-to-roll lamination in order to increase the bonding strength. The fabricated devices are compared with planar imprinted devices with regard to the cross-sectional profile of the imprinted channels and their separation functionality. The separation functionality is characterized using fluorescent polystyrene microspheres with diameters ranging from 0.5 to 5 μm.

(Some figures in this article are in colour only in the electronic version)

1. Introduction

Microfluidic lab-on-a-chip (LOC) systems for biological and chemical analysis have proven to be ideal tools for precise handling of small samples, enabling fast analysis in point-of-care and research applications (Manz *et al* 1991, Janasek *et al* 2006). Subsequently, a large number of different devices implementing valving (Oh and Ahn 2006), mixing (Nguyen and Wu 2005), metering (Haeberle and Zengerle 2007), micropumping (Laser and Santiago 2004, Woias 2004), concentration (Lin *et al* 2008) and separation (Pamme 2007) have been developed over recent decades. Many microfluidic systems are currently meeting the industrial requirements regarding stability, reliability and usability. However, an inexpensive and high-volume fabrication method is one of the remaining bottlenecks to be addressed before the systems can be commercialized in price sensitive markets—such as point-of-care diagnostics. Today, the most promising candidates for commercialization are polymer replication techniques (Abgrall and Gué 2006). Presently, the most promising commercial available candidates for fabrication of microfluidic devices are planar imprinting (hot embossing) and injection molding (Becker and Gärtner 2008) where production volumes of 100–200 devices h^{-1} have been reported (Kimerling *et al* 2006, Katoh *et al* 2008).

In this paper we demonstrate a high-volume fabrication technique for polymer microfluidic LOC systems, which is based on roll-to-roll (RtR) methods. The equipment we use is suitable for laboratory prototyping production. We have used thermal RtR nanoimprint for pattern transfer, which has been previously utilized for structuring conducting polymers (Mäkelä *et al* 2007) and optical devices (Youn *et al* 2008, Ahn and Guo 2008). In both cases the structures range in width and length from nanometers to millimeters, with imprint depths up to 1 μm. However, the channel structures in microfluidic devices are usually deeper than 1 μm. Due to

[5] Author to whom any correspondence should be addressed.

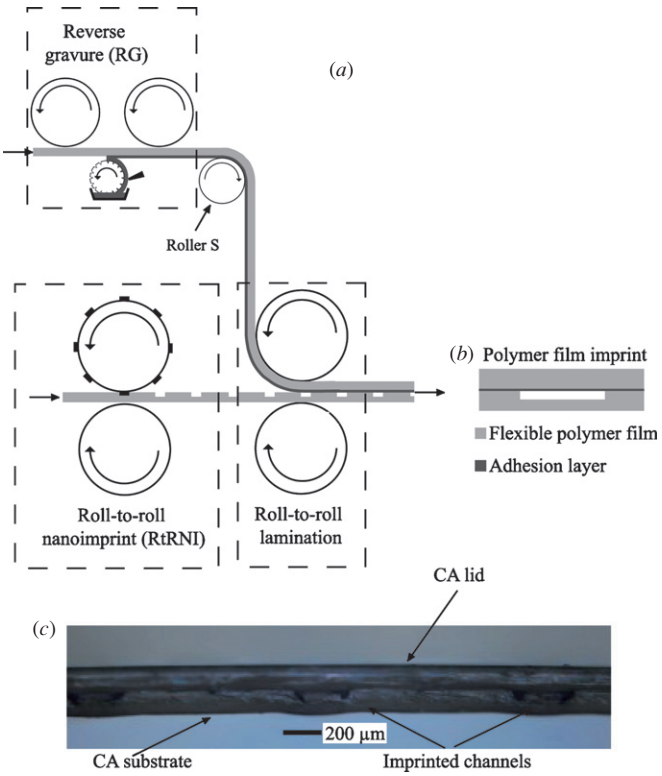

Figure 1. (*a*) Principle of RtR fabrication of microfluidic devices including reverse gravure (RG), roll-to-roll (RtR) nanoimprint and (RtR) roll-to-roll lamination. (*b*) Cross-sectional illustration of an RtR fabricated microfluidic channel. The adhesion layer is added to improve the bonding strength. (*c*) Cross-sectional image of imprinted devices. Six pairs of inlet channels are visible in the image. The adhesion layer is too narrow to be seen.

recovery effects, which arise from short imprint times, deep channels represent one of the most challenging aspects in RtR imprint. A few examples of RtR imprinting of micrometer scale structures, which are more than 1 μm deep, have been published. Examples include dots with a diameter of 10 μm, a depth of 8 μm and a pitch of 20 μm (Ishizawa *et al* 2008), and channels up to 30 μm deep and 50–100 μm wide (Ng and Wang 2009). In these publications, sealing of imprinted fluidic structures was carried out manually and not by a RtR method integrated in the production line. The high-volume production capability of RtR was therefore not exploited.

Our RtR fabrication technique consists of two parts: RtR thermal nanoimprint (RtRNI) (Mäkelä *et al* 2007, 2008, Ahn and Guo 2008) to imprint channel structures into a polymer film and RtR lamination (Kipphan 2001) to laminate another polymer film over the imprinted fluidic devices. In addition, RtR reverse gravure (RG) coating (Kipphan 2001, Kaihovirta *et al* 2008) is used to coat a smooth material layer on top of the lamination film in order to increase the bonding strength. The fabrication process is illustrated in figure 1(*a*), a cross-sectional schematic of the fabricated channels is shown in figure 1(*b*) and (*c*) is an image of an imprinted device. When the coated lamination film is guided from the RG coating to the RtR lamination, 'roller S' (see figure 1(*a*)) will be in contact with the coated surface. However, at this point the coating is dry and hard, and will not be affected by the roller. Even

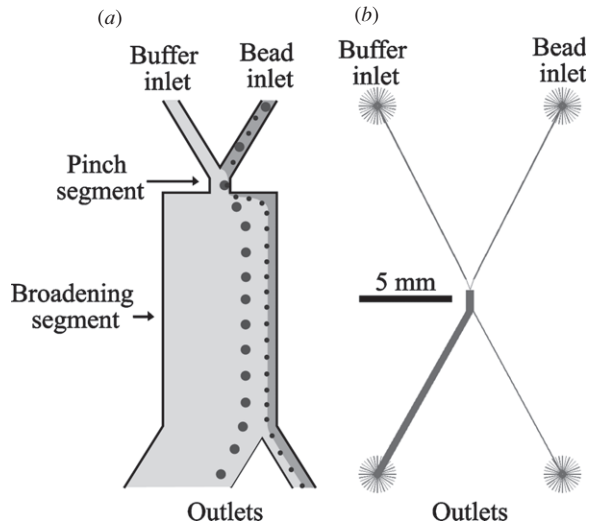

Figure 2. (*a*) Principle of PFF. (*b*) Layout of the fabricated PFF device, which has a size of 10 mm × 20 mm.

if the surface is perturbed, the RtR lamination is carried out above the glass transition temperature of the coating layer. The coating layer is thereby softened and any roughnesses or scratches that may be introduced are smoothed out and will not affect lamination strength.

As a demonstrator we have chosen a microfluidic size separation device relying on PFF (Yamada *et al* 2004). The principle of PFF is illustrated in figure 2(*a*)). Particles are separated according to their diameter by introducing two separate liquid flows, one containing particles and the other not, into another narrow channel (pinch segment). Controlling the flow rates of the two inlet channels enables alignment (pinching) of the particles to the sidewall in the narrow channel. Since the particles will follow specific streamlines, which are defined by the position of their center of mass, differently sized particles will follow different streamlines and can be separated when they move into a broader channel (broadening segment).

PFF has proven to be efficient in a number of applications such as separation of erythrocytes from blood (Takagi *et al* 2005), sub-micrometer polystyrene spheres (Sai *et al* 2006), emulsion droplets (Maenaka *et al* 2008), and recently we have demonstrated its use for detection of single nucleotide polymorphisms (Larsen *et al* 2008).

2. Experimental details

2.1. Design of the separation device

The design of the presented PFF device is shown in figure 2(*b*). In order to compare the fabrication and separation results of the RtR fabricated devices with those of devices fabricated by the established planar imprinting, the device layout is similar to the design published in previous work (Larsen *et al* 2008). The device is tailored for separation of particles ranging from 0.5 to 6 μm in diameter via channels ranging from 11.7 μm (pinch segment) to 400 μm (broadening segment) in width. All channels are 12 μm deep in order to minimize the

total volume (sample consumption) and still avoid clogging of the microspheres. In addition, particles with a diameter smaller than 4.4 μm are collected in a narrow outlet (50 μm wide) and larger particles in a wide outlet (400 μm wide), enabling downstream processing of the separated particles. This functionality has been used for DNA analysis in earlier work (Larsen *et al* 2008). However, downstream processing is not of interest in this paper. Here, separation in the broadening segment is recorded and used to evaluate the functionality of PFF. 10 mm long inlet and outlet channels ensure large separation of the inlet and outlet holes and thereby easy connection of reservoirs. The pinch and broadening segments are 20 and 1000 μm long, respectively.

2.2. Materials, fabrication and characterization methods

The polymer film used throughout the study is a 95 μm thick and 50 mm wide cellulose acetate (CA) film (from Clarifoil), and the adhesion material is Topas grade 9506 (from Topas Advanced Polymer). The glass transition temperature (T_g) of these materials is 120 °C and 60 °C respectively. Topas was dissolved in sec-buthylbenzene to a weight percentage (wt%) of 5.7 in order to obtain coating layers of 300 nm in thickness. The thickness of the adhesion layer was chosen to be much thinner than the depth of the imprinted channel structures. This is to minimize polymer flow into the channels when the lid is bonded to the imprinted structures at a temperature above the T_g of the adhesion material. A thickness of 300 nm has been proven sufficient for PFF devices fabricated by planar imprint (Larsen *et al* 2008) and was therefore chosen for RtR fabrication. A RtR RG machine (Minilabo from Yasui Seiki Co.) was applied to coat the 300 nm layer of Topas on the CA film using a 15 mm rod with 32 lines cm^{-1} at a lid speed of 0.5 m min^{-1} and a rod speed of 20 rpm. In RG coating the lid film licks the rod as indicated in figure 1(*a*). Therefore, the speed of the lid and the rod can be chosen independently. This option is convenient when the coating is combined with subsequent RtR processes as in the presented system. When Topas, dissolved in sec-buthylbenzene, was coated onto the lid film, the thickness of the layer was approximately 15 μm. A hot air curing unit, which was used to evaporate the solvent after coating, was set to 120 °C. After passing the curing unit, the dry Topas layer was 300 nm.

PFF devices were imprinted into the CA film, using a custom designed RtR imprint machine (Mäkelä *et al* 2007) at a minimum speed of 0.2 m min^{-1} The pressure between the imprint and backing roll was varied from 4.0 up to 20 MPa. A pressure of 13.6 MPa proved to give the best performance without breaking the film which was the case above 13.6 MPa. During imprint, the temperature of the imprint roll was varied from 90 °C to 125 °C while the backing roll was kept at 25 °C. Stylus profilometry (Dektak 8 Surface Profiler) was used to characterize the imprinted structures and to measure the thickness of the Topas layer on the CA lid film.

100 μm thick nickel (Ni) stamps, fabricated by electroplating on a silcone template (RTV630 from GE Silicones) with a 100 nm conductive seed gold (Au) layer, were used as shims. The silicone template was made by casting, using a silicon stamp from planar imprint as master. Nickel was electroplated onto the Au-coated silicone template in a 350 L Ni-electroplating cell (Coburn Corporation) at continuous filtering and at 45 °C. Information on the electrolyte and electrical settings are given in table 1. Detachment of the electroplated Ni-shim was done manually. Each shim, including six devices, was mechanically attached to the imprint roll.

Table 1. Process parameters for nickel electroplating.

Electrolyte	Nickel chloride	10 g L^{-1}
	Nickel content	80 g L^{-1}
	Boric acid	38 g L^{-1}
	pH	4.2
Electrical conditions	Current density	2–3 A dm^{-2}

The imprinted CA film containing the fluidic channels and the Topas coated CA film were bonded using a RtR 'office' laminator (Eagle 35 from GBC). Throughout lamination tests, the temperature between the two laminating rolls was varied from 60 °C to 100 °C, utilizing the smallest possible pressure of the machine (<0.1 MPa) to avoid deformation of the imprinted structures. The lamination speed was adjusted to match the imprint speed, which was 0.2 m min^{-1}. In general, if the imprint and lamination RtR systems are not synchronized properly, air gaps/bobbles will be trapped in between the substrate and the lid film, resulting in dysfunctional devices. However, minor sliding possibilities of the lid in the presented lamination system compensate for imprint and lamination speed variations. Therefore, perfect synchronization is not necessary in the presented system, and issues regarding lack of synchronization were not observed. After lamination, the devices were diced out and liquid access holes to the microchannels were drilled with a 1 mm glass drill. A picture of a fabricated device before access holes were drilled is shown in figure 3(*a*).

2.3. Separation measurements

In all separation measurements, fluorescent microspheres were suspended in a carrier buffer consisting of 0.001 wt% Triton X100 in MilliQ water. The microsphere concentration was 0.1 wt%. The microsphere solution was introduced into the PFF device from the bead inlet and carrier buffer without microspheres from the buffer inlet (see figure 2(*a*)). The flow rates in the bead and buffer inlet channels were 5 μL h^{-1} and 600 μL h^{-1} respectively. The flow rates were controlled by syringe pumps (11Plus from Harvard Apparatus). The separated microspheres were optically detected in the broadening segment utilizing an inverted fluorescence microscope (Eclipse2000 from Nikon) in combination with a CCD-based camera (DP253 from DeltaPix).

3. Results and discussion

To evaluate the fabricated RtR PFF devices, they have been benchmarked in regards to imprint quality and separation

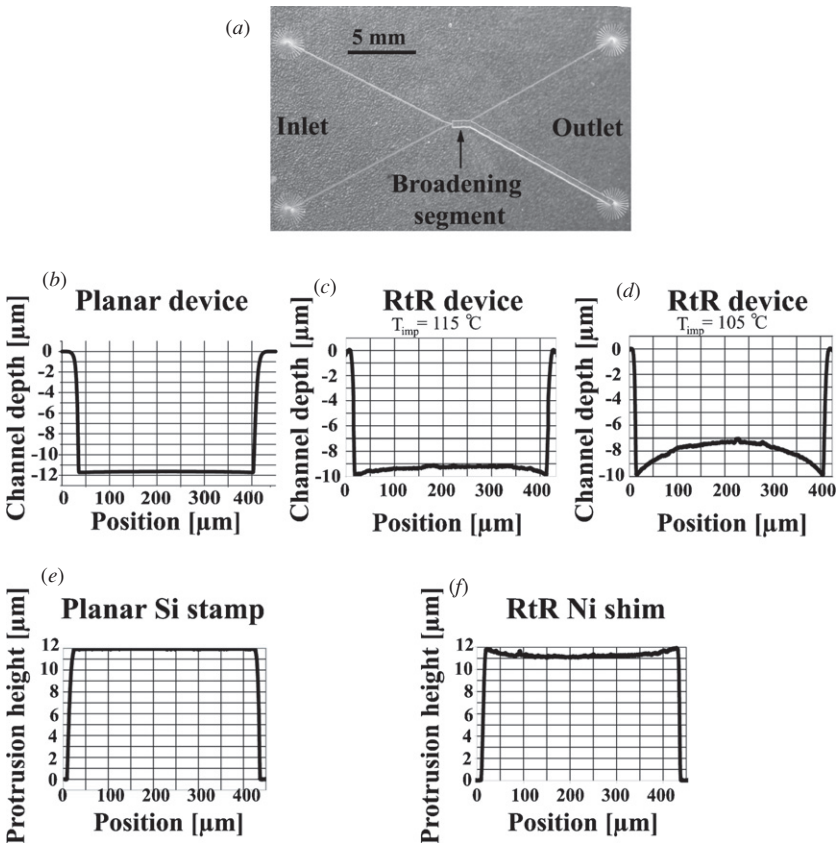

Figure 3. (*a*) Image of a RtR fabricated PFF device. (*b*)–(*d*) Surface scans of the broadening segment in a PFF device fabricated by planar (*b*) and RtR thermal nanoimprint (*c*)+(*d*). The two RtR fabricated devices are imprinted at 115 °C and 105 °C respectively, to illustrate the effect of temperature. (*e*)+(*f*) Surface scan of the broadening segment in the Si stamp and Ni shim that was used to imprint the PFF devices.

performance against similar PFF devices fabricated by planar thermal imprint in a Topas grade 8007 layer spin coated on a 4 inch silicon (Si) wafer. In this process, another 4 inch structured Si wafer was used as stamp. The fabrication scheme of planar imprinted devices is described in Larsen *et al* (2008).

3.1. Fabrication

The RtR fabrication line for making PFF devices was optimized for a production volume of 360 devices h^{-1}. At this production volume the cost per device, including material and machine usage, is approximately 0.5 euro.

Cross-sectional profilometer scans of the microfluidic channels in the planar (figure 3(*b*)) and RtR (figure 3(*c*)) fabricated devices as well as the Si stamp (figure 3(*d*)) and Ni shim (figure 3(*e*)) used to imprint the devices respectively, indicate good replication in both cases. As seen from the scan of the RtR fabricated device and the Ni shim, a small curvature in the protrusions of the Ni shim is transferred to the bottom of the channels in the RtR fabricated devices. However, this curvature is small and, as will be shown later, has negligible effect on the separation in the device. In the RtR machine, the optimized pressure, speed and temperature are found to be 13.6 MPa, 0.2 m min^{-1} and 115 °C, respectively. The imprint depth is increased up to the protrusion height at 13.6 MPa. Above this pressure the CA film breaks repeatedly due to the induced mechanical stress applied to the film. Furthermore, in order to obtain the best possible replica of the stamp features, the imprint speed has to be as low as possible; in our case this is set to 0.2 m min^{-1}. At higher imprint speeds, recovery effects in the CA result in upward curving channel floors. The imprint temperature is varied from below T_g (90 °C) to above T_g (125 °C) of CA. Below 115 °C recovery effects of the CA are significant, resulting in a curved channel floor as illustrated by an imprint at 105 °C in figure 3(*d*). Due to stretching of the CA film at imprint temperatures above T_g, 115 °C was chosen. An example of an imprint at this temperature is shown in figure 3(*c*).

In the lamination step the temperature should be higher than the T_g of the Topas adhesion layer and significantly lower than the T_g of the CA to avoid deformation of the imprinted channels. In addition, the pressure and speed should be chosen to create good contact between the adhesion layer and imprinted film without deforming the channels. The optimized lamination parameters pressure, speed and temperature are found to be 0.1 MPa, 0.2 m s^{-1} and 80 °C respectively. In some of the prepared devices poor adhesion between the Topas adhesion layer and substrate film is observed. However, the bonding is much stronger compared with samples without the adhesion layer. We did not quantitatively measure the bond and instead evaluated its quality by monitoring whether the fluid leaked during a separation measurement. None of the bondings without an adhesion layer survived the fluidic pressure, whereas approximately 75% of the devices with an

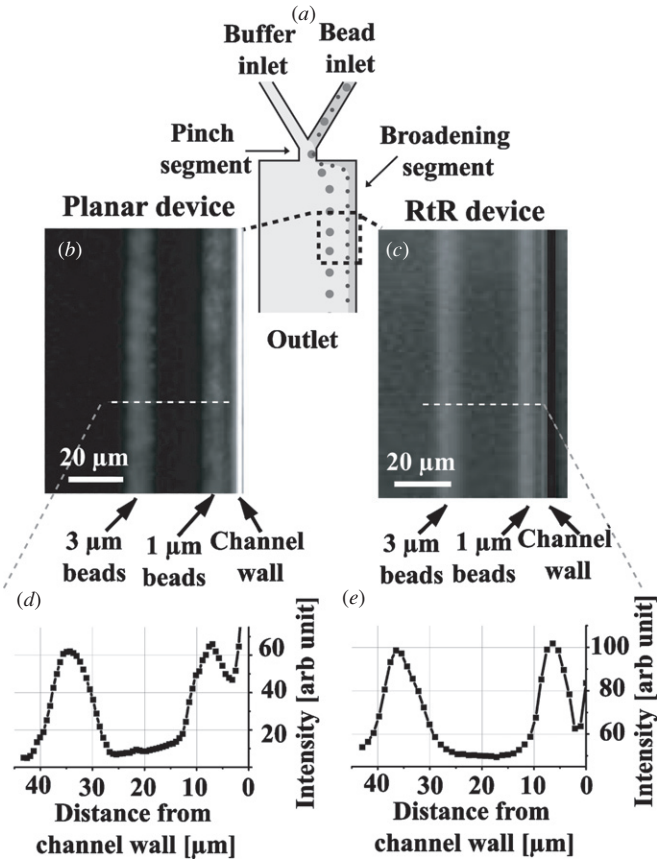

Figure 4. (*a*) Illustration of the separation principle in PFF. (*b*)+(*c*) Images of 1 and 3 μm fluorescently labeled polystyrene beads separated in a PFF device fabricated by planar and RtR thermal nanoimprint respectively. (*d*)+(*e*) Intensity scan perpendicular to the flow direction of the separated microspheres.

adhesion layer did. To enable stronger bonding and thereby a higher device yield in the future, materials with stronger adhesion should be tested.

3.2. *Separation measurements*

Separation measurements in the RtR fabricated PFF devices including microsphere diameters ranging from 0.5 to 5 μm provided similar functionality compared to the planar thermal imprinted devices as reported previously (Larsen *et al* 2008). An example of separation of 1 and 3 μm fluorescent polystyrene microspheres in planar and RtR fabricated devices is shown in the microscope images in figures 4(*b*) and (*c*), respectively.

It is seen from the microscope images in figure 4 that separation was achieved in both the planar and RtR fabricated devices. The distance from the wall in the broadening segment to the 1 and 3 μm microspheres is 7 and 34 μm respectively in the planar devices and 6 and 35 μm respectively in the RtR devices. The difference in the measured positions is within the standard deviation, which in all experiments ranged from 2 to 4 μm.

The full characterization of separation in RtR fabricated PFF devices is shown in figure 5, where the position from the

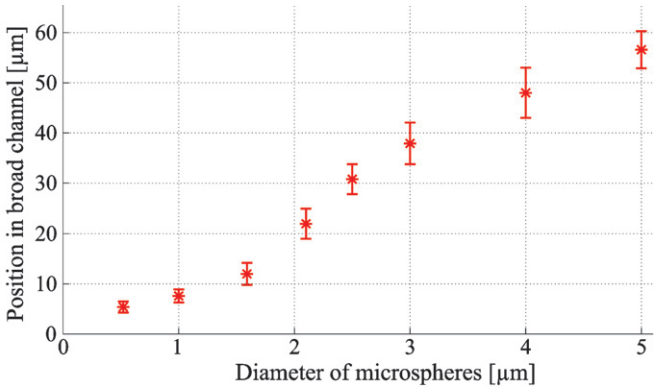

Figure 5. Separation characterization in RtR fabricated PFF devices, utilizing eight differently sized fluorescent microspheres ranging from 0.5 to 5 μm in diameter.

channel wall in the broadening segment for eight differently sized microspheres is plotted. The error bars in the plot equals two times the standard deviation of the position. From the measurements pictured in figure 5, it is estimated that up to ten differently sized spheres from 0.5 to 6 μm in diameter can be separated if the separation is only to be optically detected. Optical detection can be performed when the spatial separation of two sizes is at least the sum of the standard deviation of their position. If, on the other hand, the separated microspheres are to be collected at different outlet channels with 95% probability at two times the standard deviation, then up to six different sizes can be separated. In all presented separation measurements, the sample throughput is 5 μL h^{-1}. Combined with the microsphere concentration of 0.1 wt% and diameters ranging from 0.5 to 5 μm, this corresponds to a separation of 1.2×10^6–1.2×10^9 spheres min^{-1}.

4. Conclusion and outlook

We have presented a new high-volume fabrication scheme for polymer microfluidic LOC applications. The scheme involves two roll-to-roll methods: namely roll-to-roll nanoimprint and roll-to-roll lamination. To demonstrate the technique we have fabricated a microfluidic separation device based on pinched flow fractionation. We have optimized the fabrication line to fabricate 360 functional devices per hour at a cost of 0.5 euro per device. The fabricated separation devices were compared with planar imprinted devices by cross-sectional profilometer scans of the channels and separation of 1 and 3 μm fluorescent polystyrene microspheres. The separation functionalities of the devices were similar. In addition, the roll-to-roll fabricated devices were characterized by eight different sized microspheres, ranging from 0.5 to 5 μm in diameter.

We have used three different machines, one for each of the roll-to-roll steps. However, all the steps can, with slight machine modifications, be integrated into a single custom designed roll-to-roll imprinting machine. This would allow for a fabrication line requiring less interaction with the polymer films and higher volume production. In industrial productions this will be highly advantageous for commercialization.

Furthermore, we suggest introducing an additional imprint polymer coating with a glass transition temperature lower than that of CA, on top of the substrate CA film. As such, we show that a wide range of materials with different properties may be used by the RtR scheme, with large potential for bio-medical applications.

Acknowledgments

The authors acknowledge partial support of the EU-funded project NaPa (contract no NMP4-CT-2003-500120).

References

Abgrall P and Gué A-M 2006 Lab-on-chip technologies: making a microfluidic network and coupling it into a complete microsystem—a review *J. Micromech. Microeng.* **17** R15–49

Ahn S H and Guo L J 2008 High-speed roll-to-roll nanoimprint lithography on flexible plastic substrates *Adv. Mater.* **20** 2044–9

Becker H and Gärtner C 2008 Polymer microfabrication technologies for microfluidic systems *Anal. Bioanal. Chem.* **390** 89–111

Haeberle S and Zengerle R 2007 Microfluidic platforms for lab-on-a-chip applications *Lab Chip* **7** 1094–110

Ishizawa N, Idei K, Kimura T, Noda and Hattori T 2008 Resin micromachining by roller hot embossing *Microsyst. Technol.* **14** 1381–8

Janasek D, Franzke J and Manz A 2006 Scaling and the design of miniaturized chemical-analysis systems *Nature* **442** 374–80

Kaihovirta N J, Tobjörk D, Mäkelä T and Österbacka R 2008 Low-voltage organic transistors fabricated using reverse gravure coating on prepatterned substrates *Adv. Eng. Mater.* **10** 640–3

Katoh T, Tokuno R, Zhang Y, Abe M, Akita K and Akamatsu M 2008 Micro injection molding for mass production using LIGA mold inserts *Microsyst. Technol.* **14** 1507–14

Kimerling T E, Liu W, Kim B H and Yao D 2006 Rapid hot embossing of polymer microfeatures *Microsyst. Technol.* **12** 730–5

Kipphan H (ed) 2001 *Handbook of Print Media* (Berlin: Springer)

Larsen A V, Poulsen L, Birgens H, Dufva M and Kristensen A 2008 Pinched flow fractionation devices for detection of single nucleotide polymorphisms *Lab Chip* **8** 818–21

Laser D J and Santiago J G 2004 A review of micropumps *J. Micromech. Microeng.* **14** R35–64

Lin C-T, Kao M-T, Kurabayashi K and Meyhofer E 2008 Self-contained, biomolecular motor-driven protein sorting and concentrating in an ultrasensitive microfluidic chip *Nano Letters* **8** 1041–6

Maenaka H, Yamada M, Yasuda M and Seki M 2008 Continuous and size-dependent sorting of emulsion droplets using hydrodynamics in pinched microchannels *Langmuir* **24** 4405–10

Mäkelä T, Haatainen T, Majander P and Ahopelto J 2007 Continuous roll to roll nanoimprinting of inherently conducting polyaniline *Microelectron. Eng.* **84** 877–9

Mäkelä T, Haatainen T, Majander P, Ahopelto J and Lambertini V 2008 Continuous double-sided roll-to-roll imprinting of polymer film *Japan. J. Appl. Phys.* **47** 5142–4

Manz A, Fettinger J C, Verpoorte E, Lüdi H, Widmer H M and Harrison D J 1991 Micromachining of monocrystalline silicon and glass for chemical analysis systems—a look into next century's technology or just fasionable craze *Trends Anal. Chem.* **10** (5) 144–9

Ng S H and Wang Z F 2009 Hot roller embossing for microfluidics: process and challenges *Microsyst. Technol.* **15** 1149–56

Nguyen N-T and Wu Z 2005 Micromixers—a review *J. Micromech. Microeng.* **15** R1–6

Oh K W and Ahn C H 2006 A review of microvalves *J. Micromech. Microeng.* **16** R13–39

Pamme N 2007 Continuous flow separations in microfluidic devices *Lab Chip* **7** 1644–59

Sai Y, Yamada M, Yasuda M and Seki M 2006 Continuous separation of particles using a microfluidic device equipped with flow rate control valves *J. Chromatogr.* A **1127** 214–20

Takagi J, Yamada M, Yasuda M and Seki M 2005 Continuous particle separation in a microchannel having asymmetrically arranged multiple branches *Lab Chip* **5** 778–84

Woias P 2004 Micropumps—past, progress and future prospects. *Sensors Actuators* B **105** 28–38

Yamada M, Nakashima M and Seki M 2004 Pinched flow fractionation: continuous size separation of particles utilizing a laminar flow profile in a pinched microchannel *Anal. Chem.* **76** 5465–71

Youn S-W, Ogiwara M, Goto H, Takahashi M and Maeda R 2008 Prototype development of a roller imprint system and its application to large area polymer replication for a microstructured optical device *J. Mater. Process. Technol.* **202** 76–85